Bridge Maintenance, Safety, Management, Health Monitoring and Informatics – Koh & Frangopol (eds)

Development of an Advanced Inspection System for Weathering Steel Bridges based on Digital Image Recognition

S. Goto
Ube Machinery Corporation, Ube, Yamaguchi, Japan

T. Aso & A. Miyamoto
Graduate School of Science & Engineering, Yamaguchi University, Ube, Japan

ABSTRACT: The monitoring and condition assessment for weathering steel bridges are becoming important aspects on appropriate material selection in planning and design stages, corrosion prediction and further maintenance planning during their service life. But the visual inspection is inferior to quantitative and objective characteristics, and the dispersion of evaluation by the inspection person is wide. Therefore, the development of the new evaluation method that has high reliable, quantitative, and efficient characteristics is necessary. This paper presents the visual inspection method of rust based on image processing and pattern recognition. Three feature extraction methods; Gray level co-occurrence matrix, Fourier Transform and Multi-resolution analysis with two-dimensional wavelet decomposition characterize a representative set of 558 images. Then, SVM is used to classify a set of texture features for various corrosion levels. The classifier trained by Wavelet feature outperformed the others in terms of the identification accuracy.

1 INTRODUCTION

Non-painted bridge with weathering steel (weathering steel bridge) is a representative steel bridge that will be used in minimum-maintenance. While dryness and moisture repeating appropriately in the atmosphere, weathering steel can form adherent rust that has the quality for corrosion speed becomes slow. Therefore, if appropriate use methods and maintenance are administered, it will be the superior steel which enable bridges to be used semi-permanently in non-painted. As displayed in Figure 1, the constructive quantity of weathering steel bridges has increased considerably in Japan (Japan Association of Steel Bridge Construction 2007).

Maintenance work in order to verify the evaluation of rust conditions and the corrosion-proof performance could not be missed. The popular NDT methods such as ion transfer resistance method, electrochemical potential method, X-ray diffraction method, spectroscopic identification techniques are employed to measure the corrosion behaviors from the point of view of corrosion loss, and chemic, electric and magnetic properties of the rust patina. At present, inspection and evaluation methods of rust cannot ignore the influence of the sediment besides rust, and the system that evaluates a lot of inspection results comprehensively is not established. Therefore, there are many cases where the exterior inspection that designates the standard photograph as basis is attached importance, but the visual inspection is inferior to quantitative and objective characteristics, and the dispersion of evaluation by the inspection person is wide. The evaluation of rust conditions is an important process for the maintenance of weathering steel bridges and influences the maintenance strategy in the future. The development of the new evaluation method that has high reliable, quantitative, and efficient characteristics is necessary.

Recently, digital image recognition has been used experimentally in the automated system for bridge inspection, pavement management, sewer pipeline inspection, material engineering. The critical issues of this approach contain imaging-based feature extraction and pattern classifica-

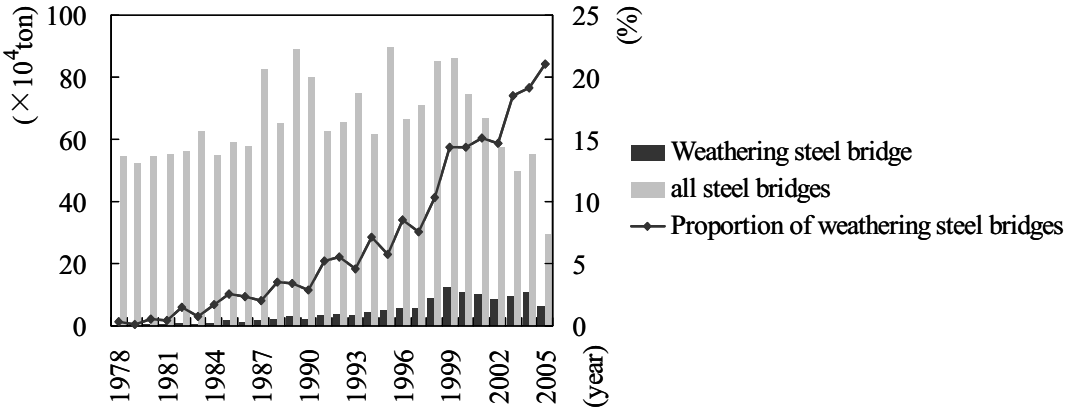

Figure 1. Constructive quantity of weathering steel bridges in Japan.

tion algorithm. The approaches for extracting textural features are very diverse, traditional approaches such as Gray Level Co-occurrence Matrix (GLCM) methods, transform-based approaches based on Fast Fourier Transform (FFT) and Wavelet Transform (WT). The WT analysis has shown better performance in many cases due to its outstanding capabilities in space-frequency decomposition at different scale. Another crucial issue is the pattern classification, numerous classifiers using the extracted features have been employed, including nearest neighbor classifier, Bayes classifier, probabilistic neural network, and learning vector quantization. Recently, the support vector machine (SVM) is becoming a successful method for pattern recognition.

This paper presents the visual inspection method of rust based on image processing and pattern recognition. Three feature extraction methods; GLCM, FFT and WT characterize a representative set of 558 images. Then, SVM is used to classify a set of texture features for various corrosion levels. The classifier trained by Wavelet feature outperformed the others in terms of classification rate.

2 VISUAL INSPECTION BASED CONDITION ASSESSMENT

Japan Association of Steel Bridge Construction and Japan Iron and Steel Federation proposed the visual inspection based criterion for condition assessment of weathering steel. As shown in Table 1, the condition states are categorized into 5 levels ranging from 5 to 1. The rust patina with an average granule size of smaller than 5mm diameter is rated as acceptable, while the rust flakes with granule sizes in the range of 5mm ~ 25mm diameter indicate the requirement of detail inspection. The very poor condition state, i.e. level 1 implies the area observed having thick and loose laminar sheets is failed completely and appears very severe corrosion. Besides the texture, the color of the rust patina is also highlighted in rating. As displayed in Figure 2, 6 representative sample images of weathering steel specimen extracted from 9 years' exposure tests on 41 weathering steel bridges around in Japan are used as references for practical rating. The variations of color and texture of images with respect to condition state can be clearly observed. Note that the pro-posed criterion requires expert or trained staff to use subjective judgment on variations of color and texture properties for decision-making. Moreover, to promote the capabilities of the method for quantitative analysis, the thickness measurement on the rust layer is suggested as an indispensable supplement. As shown in Table 1, when the rust thickness is smaller than 400μm, its condition state can be viewed as acceptable. Generally, the electromagnetic coating thickness tester is applied to quantitative thickness measurement.

It is evidence that the visual inspection based condition assessment approaches are still time-consuming and subjective. The current study is to develop image processing and pattern classification techniques to conduct a quantitative assessment on the condition state of corroded weathering steel bridges.

Table 1. Rating criterion based on visual inspection and rust thickness measurement.

Condition state	Attribute	Description of rust patina	Rust thickness
5	Acceptable	Very thin protective oxide film	< 200μm
4		Average granule size: <1mm diameter	< 400μm
3		Average granule size: 1~5mm diameter	
2	Require detail inspection	Granule size: 5~25mm diameter Having rust flakes	> 400μm < 800μm
1	Failed	Thick and loose laminar sheets, very severe corrosion	> 800μm

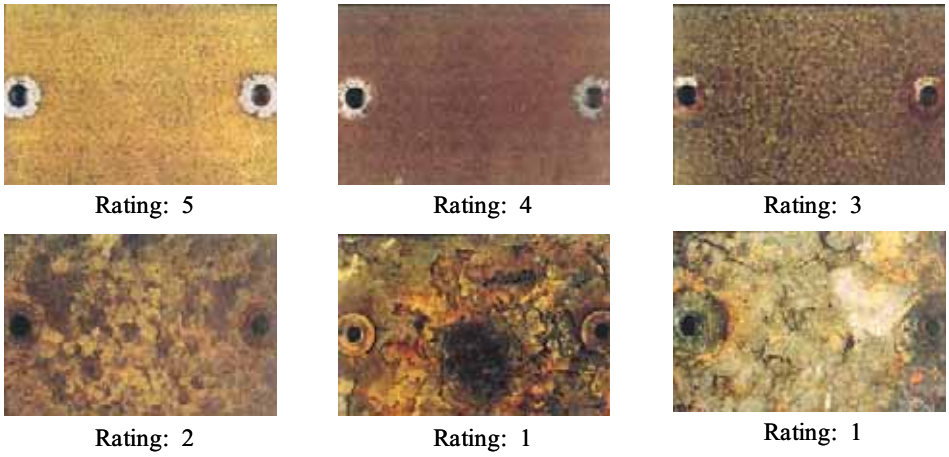

Figure 2. Appearance of 9 years' exposure test on weathering steel specimen and the corresponding rating results via visual inspection (specimen size: 150mm×100mm).

3 FEATURE EXTRACTION BASED ON IMAGE PROCESSING

3.1 *Gray Level Co-occurrence Matrix*

GLCM is representative of the statistical approaches to texture analysis. The GLCM of an image is an estimate of the second-order joint probability, $P_\delta(i,j)$ of the intensity values of two pixels (i and j), a distance δ apart along a given direction θ, i.e., the probability that i and j have the same intensity. This joint probability takes the form of a square array P_δ, with row and column dimensions equal to the number of discrete gray levels (intensities) in the image being examined. If an intensity image were entirely flat (i.e. contained no texture), the resulting GLCM would be completely diagonal. As the image texture increases (i.e. as the local pixel intensity variations increase), the off-diagonal values in the GLCM become larger.

A quantitative analysis of the GLCM has been proposed through 14 textural descriptors calculated by P_δ. In this study, four of the most commonly used descriptors (angular second moment, contrast, correlation, and entropy) are used to extract textural features from GLCMs.

$$ASM = \sum_{i=0}^{n-1}\sum_{j=0}^{n-1}\{P_\delta(i,j)\}^2 \tag{1}$$

$$CON = \sum_{i=0}^{n-1}\sum_{i=0}^{n-1}(i-j)^2 P_\delta(i,j) \tag{2}$$

$$COR = \left\{\sum_{i=0}^{n-1}\sum_{j=0}^{n-1} ijP_\delta(i,j) - \mu_x\mu_y\right\} \Big/ \sigma_x\sigma_y \tag{3}$$

$$ENT = -\sum_{i=0}^{n-1}\sum_{j=0}^{n-1} P_\delta(i,j)\log\{P_\delta(i,j)\} \tag{4}$$

Here the means and variances in the x and y direction are given by

$$\mu_x = \sum_{i=0}^{n-1} i\sum_{j=0}^{n-1} P_\delta(i,j), \quad \mu_y = \sum_{j=0}^{n-1} j\sum_{i=0}^{n-1} P_\delta(i,j) \tag{5}$$

$$\sigma_x = \sum_{i=0}^{n-1} (i-\mu_x)^2\sum_{j=0}^{n-1} P_\delta(i,j), \quad \sigma_y = \sum_{j=0}^{n-1} (j-\mu_y)^2\sum_{i=0}^{n-1} P_\delta(i,j) \tag{6}$$

3.2 *Fourier transform*

The two-dimensional Fast Fourier Transform (2-D FFT) of an image can be thought of as a two-dimensional representation of the spatial power spectrum of the image. Theoretical details regarding the 2-D FFT can be obtained from the image-processing literature and many researchers have proposed the use of FFT spectra as texture feature descriptors. In this study, the commonly used descriptor is used to extract textural features from FFT spectra.

$$d(r') = \int_0^{2\pi} \left|F(r',\theta)\right|^2 d\theta \tag{7}$$

Here $F(r',\theta)$ is Fourier spectrum in polar coordinates system, r' is the distance from the center of FFT spectra map, and θ is the central angle. The center of FFT spectrum map is the direct current, and as r' is far from the center, the frequency component is higher. Then, $d(r')$ is an estimate of the frequency energy at each level. In this study, the ratio of the frequency energy is proposed as follow:

$$R_{r'} = \frac{d(r')}{\sum d(r')}; \quad r' = 100,200,...,500 \tag{8}$$

3.3 *Wavelet transform*

Whereas the 2-D FFT performs a frequency decomposition of an image, the 2-D wavelet transform performs a space-frequency decomposition, which is more suitable for texture analysis. The wavelet energy signatures reflecting the distribution of energy along the frequency domain over scale and orientation are often employed as the texture features. To eliminate the effect of illumination intensity, the normalized energy vector is used to describe the energy distribution at each level (Shin & Hryciew 2004).

$$E_i^n = \frac{E_{LH_i} + E_{HL_i} + E_{HH_i}}{\sum_{m=1}^{k}(E_{LH_m} + E_{HL_m} + E_{HH_m})} \tag{9}$$

Here E_i^n is the normalized energy distribution at the decomposition level i, k is the largest decomposition level, E_{LH_m}, E_{HL_m}, E_{HH_m} are respectively the energy of the detail subimages LH_m, HL_m, HH_m at level m. Three sub-images (LH, HL, and HH) respectively related to low-high (vertical), high-low (horizontal), high-high (diagonal) frequency sub-bands denote the finest scale wavelet coefficients, namely, detail images. Note that for each subimage with $M \times N$ pixels at that level, the energy can be, for instance, in the case of low-high (LH) orientation, expressed as

$$E_{LH_m} = \sum_{M,N} \left|C_{LH_m}(x,y)\right|^2 \tag{10}$$

For the rust patina of weathering steel under acceptable condition states of 3, 4 and 5 shown in Figure 2, its surface image appears appropriate to be described by the normalized wavelet energy distribution due to its having relative small and uniform compact granule. While in the states of 1 and 2, the corroded surface image shows severe irregularity. Its texture content in each scale showing strong local characteristics should be captured both in global and local distribution of the energy. In this study, a simple method partially considering the local texture content is proposed as follow:

$$E_i^l = \frac{E_{HH_i}}{E_{LH_i} + E_{HL_i}} \tag{11}$$

Here E_i^l represents the ratio of the energy in the diagonal direction to the addition of that in vertical and horizontal directions. Hence, a texture feature vector can be constructed in the form

$$E = (E_1^n, E_2^n, \ldots, E_k^n, E_1^l, E_2^l, \ldots, E_k^l) \tag{12}$$

4 PATTERN CLASSIFICATION BASED ON SUPPORT VECTOR MACHINE

Recently, an emerging pattern classification method termed support vector machine (SVM) has received a great deal of attention and demonstrated excellent performance in terms of pattern classification. The basic concept of SVM is to transform the data set to a high dimensional kernel-induced feature space and determine the separating hyperplane that has maximum distance to the closest points of the training set. The success of SVM is attributed to its employing the structural risk minimization principle rather than the commonly used empirical risk minimization in artificial neural network. Thus the idea of SVM is to determine a classifier which minimizes a bound on the generalization error instead of simply minimizing the training error. In addition, the SVM training will be equivalent to solving a quadratic programming problem. Consequently, the solution is always unique and globally optimal. A brief introduction of the broadly applied models of SVM namely maximal margin classifier and soft margin classifier is presented here.

Consider a linearly separable training set S be $\{(\mathrm{x}_1, y_1), \ldots (\mathrm{x}_n, y_n)\}$ where $\mathrm{x}_i \in R^{\mathrm{D}}$ is a $\mathrm{D}-$dimensional vector of input attributes and R is the corresponding output label. The SVM requires to solve nonlinear classification problem in the form

$$\begin{aligned} \min_{\mathrm{w}, b, \xi} \quad & \langle \mathrm{w} \cdot \mathrm{w} \rangle + C \sum_{i=1}^{n} \xi_i \ , \\ \text{subject to} \quad & y_i \left(\langle \mathrm{w} \cdot \Phi(\mathrm{x}_i) \rangle + b \right) \geq 1 - \xi_i , \\ & \xi_i \geq 0. \end{aligned} \tag{13}$$

Here $\xi_i,\ i = 1, \ldots, n$ are the slack variables and C is a penalty parameter used in the margin constraints to promote the robust measure of the margin distribution. For nonlinear case, a kernel function $K(\mathrm{x}_i,\ \mathrm{x}_j) = \langle \Phi(\mathrm{x}_i), \Phi(\mathrm{x}_j) \rangle$. is introduced to map the low-dimension input space R^d to high-dimension feature space F using the nonlinear function Φ, i.e. $z_i = \Phi(\mathrm{x}_i)$. There are many possible choices of the kernel functions such as linear, polynomial, radial basis function (RBF), and sigmoid function. In the present study, the RBF kernel (Gaussian kernel) with kernel parameter γ controlling its width given by the follow is used.

$$K(\mathrm{x},\ \mathrm{y}) = \exp(-\gamma \| \mathrm{x} - \mathrm{y} \|^2) \tag{14}$$

Hence, there are two parameters C and γ having effect on the performance of SVM.

5 EXPERIMENTS

5.1 *Flow chart*

A schematic of the advanced inspection system for weathering steel using image processing and SVM is shown in Figure 3. The surface image data of weathering steel acquired by digital camera were preprocessed to create standard rescaled grayscale image for image processing. Then, the SVMs were implemented to classify a set of texture features into various corrosion levels related to condition state of the surface images of weathering steel. The quality assessment was finally reported. In this study the LIBSVM toolbox is employed for classification (Hsu et al., 2003).

5.2 *Image acquisition*

As earlier stated that the following classification and comparison of the image texture are strongly scale dependent, consequently, to determine the magnification and resolution of the original image, the image acquisition starts by placing two square sheets with grid points marked and a distance of 30cm on the imaged surface. Two types of images with 2048×1536 and 2560×1920 pixels were acquired. Once the image resolution was known, the image rescaling was implemented to ensure each image having the same resolution of $1650/30 = 55$ pixel/cm. Then, a set of 558 images each with a size of 1024×1024 pixels were split from the rescaled images and transformed to 256 grayscale images for further texture analysis. To compare the performance of the proposed system with that of the traditional visual inspection method for classification, the condition state of each image was rated according to the criteria shown in Table 1 and Figure 2 by experienced inspector. The electromagnetic coating thickness tester is utilized to measure the thickness of the loose rust patina as a complementary for rating.

5.3 *Training and testing samples*

With the created grayscale images, texture features are extracted using the image processing. Table 2 shows texture features from each processing method of an image data set with their number of dimensions. GLCMs is calculated from four displacement vectors $\theta = 0^\circ, 45^\circ, 90^\circ$, and 135°, and used their average. The scale of the displacement vector is chosen to be 10, 20, or 50 pixels. Wavelet texture features are calculated using the coif1 wavelet basis, and the rescaled image is decomposed with level equals to 6. To check the robustness of the SVM in dealing

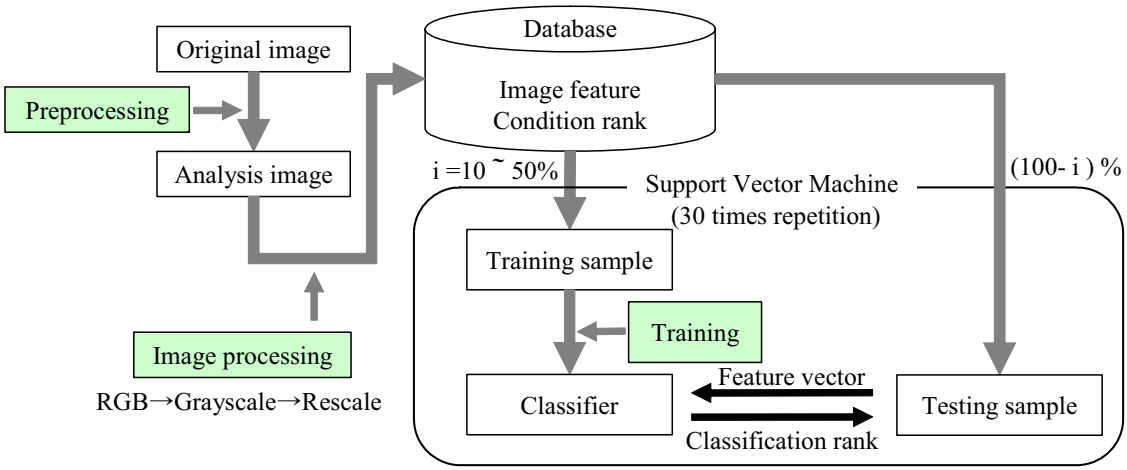

Figure 3. Imaging-based condition rating of weathering steel using SVM.

with problems with limited training samples, a faction of the total texture feature vectors of the images ranging from 10% to 50% are employed to train the SVM classifier, while the rest are used for testing. Another critical issue is to consider the randomness of the training and testing procedures. In this study, for each case with different texture features and partition percentages of training and test sets, 30 times of classification procedure are randomly conducted using cross-validation method and all the identification accuracies are averaged to evaluate the SVM classifiers.

5.4 *Experimental results*

Figure 4 shows the averaged identification accuracy in each case. Comparison of each accuracy shows the classifier trained by Wavelet feature outperformed the others. On the other hand, the classifier trained by GLCM and FFT features of case3 has much the same accuracy as trained by Wavelet feature in training images (50%), but it is not sufficient in comparison with the number of dimensions. Although considering both of GLCM which gives local statistical features and FFT which gives global frequency features, it can not be trained effectively.

In wavelet analysis, note that the decomposition level is an important issue and has unavoidable effect on the further classification. In order to investigate the performance of the wavelet texture features in different decomposition levels, the rescaled image is decomposed with level equals to 5, 6, 7, and 8. Figure 5 shows the averaged identification accuracy in the case of each decomposition level. As can be seen, with the increase of the decomposition level, the averaged identification accuracy has the trend of increase. When the half samples are used for training in level 7, the best classification results (about 87%) can be obtained. However, in the case of levels 6, 7 and 8, the variation appears to be very small. The wavelet feature in low decomposition level analysis is low dimension, and enhances the confidence level on condition that classifying by same samples. Moreover, the calculation time for wavelet analysis and training by SVM can be reduced, and it can be thought that the optimum decomposition level is 6 for identification.

Table 2. Image feature and dimension.

Case	Image processing	Feature	Dimension
1	GLCM	*ASM,CON,COR,ENT (r=10,20,50)*	12
2	FFT	*Rr' (r' = 100 ~500)*	5
3	Case1 and Case2		17
4	WT	*E*	12

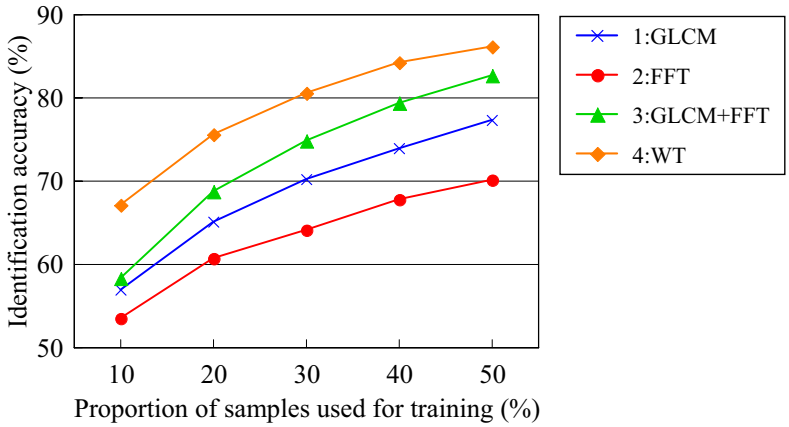

Figure 4. Averaged identification accuracy.

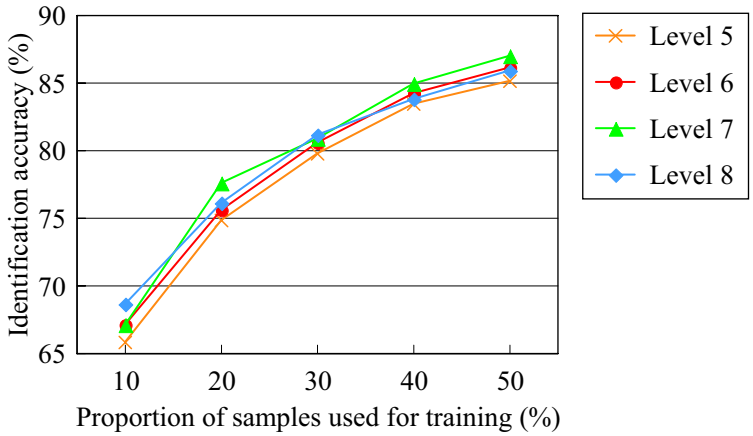

Figure 5. Averaged identification accuracy in the case of each decomposition level.

Table 3. Classification result of 50% training images in the case of level 6.

Rating	Identification result					Sum
	1	2	3	4	5	
1	1,213 (94)	14 (1)	63 (5)			1,290 (100)
2	44 (2)	1,774 (86)	191 (9)	16 (1)	45 (2)	2,070 (100)
3	84 (4)	312 (16)	1,395 (72)	152 (8)	7	1,950 (100)
4		10 (1)	97 (6)	1,575 (92)	28 (1)	1,710 (100)
5	4	70 (5)	4	24 (2)	1,218 (93)	1,320 (100)

Number (%)

Table 3 shows the total of classification results of 50% training images and 30 classifications in the case of level 6. The Rating-1 image has the best accuracy 94%, and the lowest accuracy is 72% in the Rating-3 image. They are high accurate classifications, and the proposed inspection system for weathering steel using image processing and SVM can be realized efficiently.

6 CONCLUTIONS

In this paper, we proposed the advanced inspection system based on image processing and SVM for weathering steel bridges. Three feature extraction; GLCM, FFT and WT characterize a representative set of 558 images, and SVM is used to classify a set of texture features for various corrosion levels.

Comparison of each accuracy shows the classifier trained by Wavelet feature outperformed the others. Investigating the performance of the wavelet texture features in different decomposition levels, the variation appears to be very small in the case of levels 6, 7 and 8. Hence, it can be thought that the optimum decomposition level is 6 for identification. They are high accurate classifications, and the proposed inspection system can be realized efficiently.

REFERENCES

Hsu, C. W., Chang, C. C. & Lin, C. J. 2003. A practical guide to support vector classification. Available at www.csie.ntu.edu.tw/~cjlin/libsvm.

Shin, S. & Hryciew, R. D. 2004. Wavelet analysis of soil mass images for partical size determination. *J. Comput. Civ. Eng.* 18(1): 19-27.

The Kozai Club (Iron and Steel Mill Products Association) and Japan Association of Steel Bridge Construction. 2001. *Application of Weathering Steel to Highway Bridges (Explanation)*.